/

Article / Book Information

Title	Characterization of Half-Metallic L2_1_-Phase Co_2_FeSi Full-Heusler Alloy Thin Films Formed by Rapid Thermal Annealing
Authors	Y. Takamura,R. Nakane,H. Munekata,S. Sugahara
Citation	J. Appl. Phys., vol. 103, no. 7,
/Pub. date	2008, 4
/Journal home page	http://jap.aip.org/
/Copyright	Copyright (c) 2008 American Institute of Physics

Characterization of half-metallic $L2_1$-phase Co$_2$FeSi full-Heusler alloy thin films formed by rapid thermal annealing

Yota Takamura,[1,a)] Ryosho Nakane,[2] Hiro Munekata,[1,3] and Satoshi Sugahara[1,3,b)]

[1]*Department of Electronics and Applied Physics, Tokyo Institute of Technology, Yokohama 226-8502, Japan*
[2]*Department of Electronic Engineering, The University of Tokyo, Tokyo 113-8656, Japan*
[3]*Imaging Science and Engineering Laboratory, Tokyo Institute of Technology, Yokohama 226-8502, Japan*

The authors developed a preparation technique of Co$_2$FeSi full-Heusler alloy thin films with the $L2_1$-ordered structure on silicon-on-insulator (SOI) substrates, employing rapid thermal annealing (RTA). The Co$_2$FeSi full-Heusler alloy films were successfully formed by RTA-induced silicidation reaction between an ultrathin SOI (001) layer and Fe/Co layers deposited on it. The highly (110)-oriented $L2_1$-phase polycrystalline full-Heusler alloy films were obtained at the RTA temperature of 700 °C. Crystallographic and magnetic properties of the RTA-formed full-Heusler alloy films were qualitatively the same as those of bulk full-Heusler alloy. The proposed technique is compatible with metal source/drain formation process in advanced complementary metal-oxide semiconductor technology and would be applicable to the fabrication of the half-metallic source/drain of metal-oxide-semiconductor field-effect transistor type of spin transistors. © *2008 American Institute of Physics.* [DOI: 10.1063/1.2838648]

In recent years, spin transistors[1–4] attract considerable attention, since they have interesting transistor behavior with a new degree of freedom in controlling output currents based on spin-related phenomena. This feature makes it possible that spin transistors have useful nonvolatile and reconfigurable functionalities to improve circuit performance beyond present transistors. However, high current drive capability and a large on/off current ratio are still important requirements even for spin transistors, as well as present ordinary transistors.[4] In addition, excellent scalability and integration ability are also indispensable to establish very large scale integration. From these points of view, one of the promising spin transistors is recently proposed spin metal-oxide-semiconductor field-effect transistors (spin MOSFETs).[3,4] The basic structure of spin MOSFETs consists of a MOS capacitor and ferromagnet contacts for the source and drain, and the device performance depends on the material of the ferromagnetic source/drain. Half-metallic ferromagnets[5] (HMFs) are the most effective source/drain material to realize the spin-dependent output characteristics of spin MOSFETs,[3,4] owing to their extremely high spin polarization and unique spin-dependent band structure.

Recently emerging silicide-based metal source/drain MOSFET (Ref. 6) technology would be applicable to the fabrication of spin MOSFETs, due to the similarity in the device structure between metal source/drain MOSFETs and spin MOSFETs. For metal source/drain MOSFETs, transition metal (or rare earth metal) silicides are directly used as their source and drain. These silicides are formed by thermally activated intermixing reaction, the so-called silicidation, between a Si substrate and transition metal (or rare earth metal)

layer deposited on the Si substrate. In general, the thermal process for silicidation is induced by rapid thermal annealing (RTA). $L2_1$-phase half-metallic full-Heusler alloys containing Si (Co$_2$FeSi,[7,8] Co$_2$MnSi,[9] etc.) are one of attractive candidates for spin MOSFETs with the HMF source/drain, since these materials are considered to be a kind of silicides and thus they have a possibility to be formed by the RTA-induced silicidation process. In this paper, we developed a RTA-induced silicidation technique to form $L2_1$-phase Co$_2$FeSi full-Heusler alloy films, utilizing a silicon-on-insulator (SOI) substrate. Magnetism in the RTA-formed Co$_2$FeSi full-Heusler alloy films is also discussed.

The problem of the RTA technique for ferromagnetic silicides including Si-containing full-Heusler alloys is the formation of nonmagnetic silicides with low magnetic element content. This is caused by the deep diffusion of magnetic elements into a Si substrate. In other words, when the much amount of Si atoms is supplied from the Si substrate, the most thermodynamically favorable nonmagnetic silicides are preferentially formed. Figure 1 shows the proposed preparation method of full-Heusler alloys employing a SOI substrate. The diffusion of magnetic atoms is blocked by the buried oxide (BOX) layer of the SOI substrate, and thus the composition of the RTA-formed film layer can be easily controlled by the thickness of the magnetic metal and SOI lay-
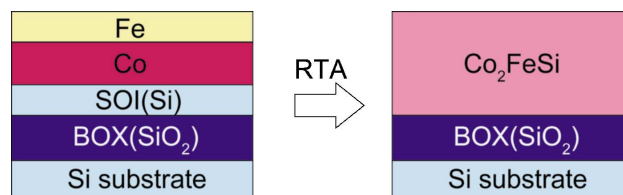

FIG. 1. (Color online) Schematic illustration of Co$_2$FeSi (CFS) formation process using a silicon-on-insulator (SOI) substrate.

a)Electronic mail: yota@isl.titech.ac.jp.
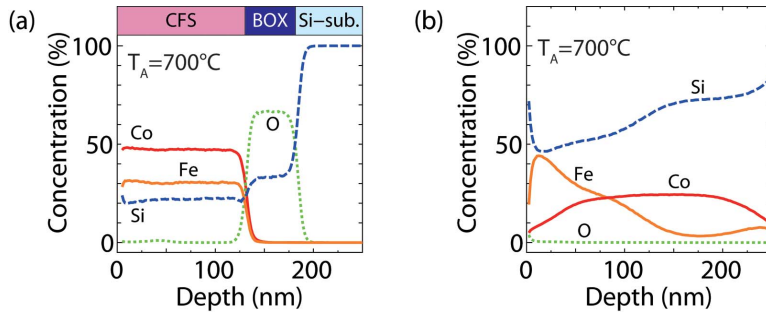b)Electronic mail: sugahara@isl.titech.ac.jp.

FIG. 2. (Color online) SIMS depth profiles of Co, Fe, Si, and O (a) in a RTA-treated Fe/Co/SOI/BOX/Si sample and (b) in a RTA-treated Fe/Co/Si sample.

ers. When the amount of constituent elements of the resulting film layer is limited (or adjusted) to the chemical composition of full-Heusler alloys, homogeneous full-Heusler alloys would be formed, since full-Heusler alloys are also one of thermodynamically stable phases as long as keeping their (near) stoichiometric composition. Recently, ferromagnetic Fe_3Si that has the $L2_1$-related DO_3 structure was successfully formed by this technique.[10]

All the experiments were carried out using commercially available wafer-bonding SOI substrates that consist of a thin SOI layer, BOX layer, and Si substrate (hereafter, this structure is referred to as SOI/BOX/Si). A SOI substrate sample was cleaned by chemical oxidation using H_2SO_4 and H_2O mixture and successive etching of the resulting surface oxide by buffered HF solution. Then Co and Fe films were deposited on the SOI layer surface in an ultrahigh vacuum. Subsequently, silicidation was performed by RTA in N_2 atmosphere. The thicknesses of Co and Fe films were measured by an uncalibrated quartz oscillator thickness monitor. The sample structure and a central experimental condition were as follows: the SOI thickness d_{SOI} of 40 nm, the Co thickness d_{Co} of 45 nm, the Fe thickness d_{Fe} of 24 nm, the annealing temperature T_A of 700 °C, and the annealing time t_A of 4 min. These parameters were used throughout the following experiments, unless otherwise noted. Hereafter, Co_2FeSi will be expressed as CFS even for off-stoichiometric composition.

Figure 2(a) shows depth profiles of Co, Fe, Si, and O in a RTA-treated Fe/Co/SOI/BOX/Si sample. The depth profiles were measured by secondary ion mass spectroscopy (SIMS) with the MCs^+ technique,[11] and the SIMS intensity of each element was calibrated by Rutherford backscattering and particle induced x-ray emission measurements. As expected, the diffusion of Co and Fe was completely blocked by the BOX layer, and the Co, Fe, and Si concentrations in the RTA-formed film exhibited plateau profiles. The concentrations of Co, Fe, and Si were 48%, 30%, and 22%, respectively, which was slightly off-stoichiometric composition. The deviation from the stoichiometric composition would be caused by the uncalibrated quartz oscillator thickness monitor. On the other hand, when the silicidation was performed using an ordinary Si substrate instead of a SOI substrate, Fe and Co were much deeply diffused into the Si substrates, as shown in Fig. 2(b).

The crystallographic features of the RTA-formed CFS film were characterized by x-ray diffraction (XRD). After the Fe/Co/SOI/BOX/Si sample was annealed at T_A=700 °C, the RTA-formed film showed strong CFS (220) and (440)

diffraction peaks and no other diffraction peaks of CFS were observed in the 2θ range between 20 ° and 120°, indicating that the RTA-formed CFS thin film was highly (110) oriented. Note that the lattice constant of the CFS film was 0.5636 nm, which was slightly smaller than that of the bulk value (0.5647 nm).[12] The deviation of the lattice constant from the bulk value would be caused by the off-stoichiometric composition. When an ordinary Si substrate was used, the sample showed no CFS-related diffraction peak, as shown by the top curve in Fig. 3(a). These results were consistent with the above-described SIMS observations. The thermally activated silicidation process in the CFS formation was also traced by XRD measurements. The results are also shown in Fig. 3(a). An as-deposited Fe/Co/SOI/BOX/Si sample showed no diffraction peak at around the CFS (220) diffraction ($2\theta \sim 45.6°$). When the sample was annealed at T_A=400 °C, a diffraction peak newly appeared at 2θ=45.0°, which was slightly smaller than the peak position of the CFS (220) diffraction. This diffraction peak can be assigned by $Co_9Fe_9Si_2$ (110) or $FeSi_2$ (421), indicating insufficient silicidation reaction. The diffraction of CFS (220) started to be observed at T_A=600 °C, resulting in the bimodal shape of the diffraction pattern, i.e., the film contained at least two crystalline phases. Above T_A=700 °C, the diffraction peak at 45.0 ° was vanished. Only the CFS (220) diffraction was clearly observed and no other obvious diffraction peaks were detected, as described above. When the direction normal to the sample plane was inclined toward 45° and 35.3° from the x-ray-source-detector-sample
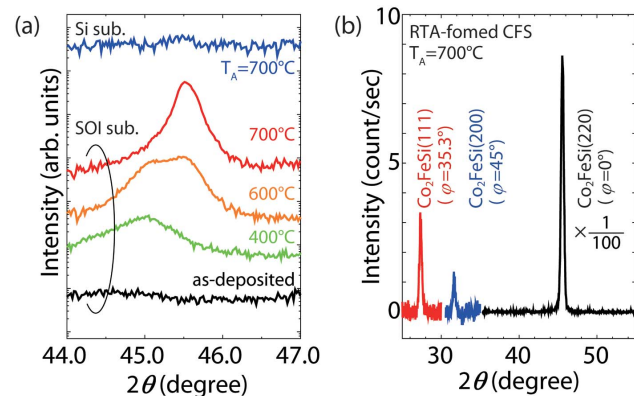

FIG. 3. (Color online) (a) XRD patterns of the RTA-treated Fe/Co/SOI/BOX/Si samples with various RTA temperatures (T_A). The XRD pattern of a RTA-treated Fe/Co/Si sample is also shown as a reference (topmost XRD pattern). (b) Superlattice diffraction of the RTA-formed CFS film. φ is the tilted angle of the sample plane.
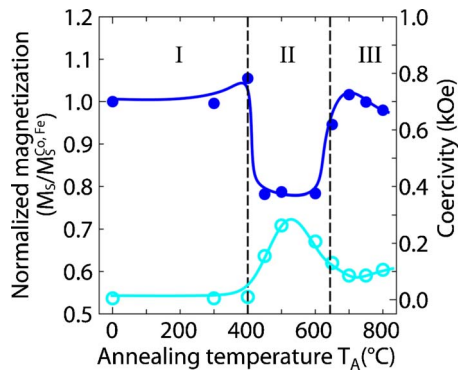
FIG. 4. (Color online) Magnetization $M_S/M_S^{\mathrm{Co,Fe}}$ (solid circles) and coercivity H_C (open circles) as a function of RTA temperature T_A for the RTA-formed CFS samples.

FIG. 5. (Color online) MCD spectra of the RTA-formed CFS film with T_A = 700 °C (solid line) and reference samples (the others).

plane, the CFS (200) and (111) diffractions indicating fully ordered $L2_1$ structures were clearly observed for the RTA-formed CFS film, as shown in Fig. 3(b). Therefore, the formation of highly (110)-oriented $L2_1$-ordered CFS films was confirmed to be successfully formed by RTA-induced silicidation, using a SOI substrate.

Figure 4 shows the saturation magnetization M_S and coercivity H_C of the RTA-formed CFS thin films as a function of T_A, where M_S was normalized by the saturation magnetization $M_S^{\mathrm{Co,Fe}}$ of their as-deposited sample. The measurements were carried out using a superconductive quantum interference device (SQUID) magnetometer at 300 K. All the data were taken with a magnetic field applied parallel to the in-plane direction of the SOI (001) substrate. The changes in M_S and H_C can be divided into three regions, as noted in the figure. In region I (300 °C $\leqslant T_A \leqslant$ 400 °C), $M_S/M_S^{\mathrm{Co,Fe}}$ maintained almost unity and H_C little changed, indicating that there is no detectable silicidation reaction. In region II (400 °C $\leqslant T_A \leqslant$ 650 °C), M_S rapidly decreased and took a minimum value. This implies that the thermally activated silicidation process proceeded, and that the formation of nonmagnetic silicides, such as $FeSi_2$, reduced $M_S/M_S^{\mathrm{Co,Fe}}$. In this region, H_C took a maximum value at around $T_A = 500$ °C, and then deceased with increasing T_A, which would also reflect the uniformity of the film. In region III (650 °C $\leqslant T_A \leqslant$ 800 °C), M_S increased to $M_S^{\mathrm{Co,Fe}}$ and then was slightly reduced with increasing T_A. In this region, H_C took an almost constant value of 89 Oe. In addition, the *M-H* curves of the samples were a single-step squarelike hysteresis loop with sharp magnetization switching. These results mean that when the $L2_1$-phase CFS film was formed, the magnetic properties were drastically improved. The magnetic moment per unit cell of the sample in region III was $5.2\mu_B - 4.8\mu_B$, which is slightly smaller than the bulk value $(6\mu_B)$.[8] This might be caused by the deviation of chemical composition from stoichiometric CFS, and by the incorporation of oxygen during RTA.

A solid curve in Fig. 5 shows the magnetic circular dichroism (MCD) spectrum of the RTA-formed CFS film $(T_A = 700$ °C). MCD spectra for its as-deposited Fe/Co/SOI/BOX/Si sample, an as-deposited Co/SOI/BOX/Si sample, and a RTA-treated Fe/Co/SiO$_2$/Si sample with T_A
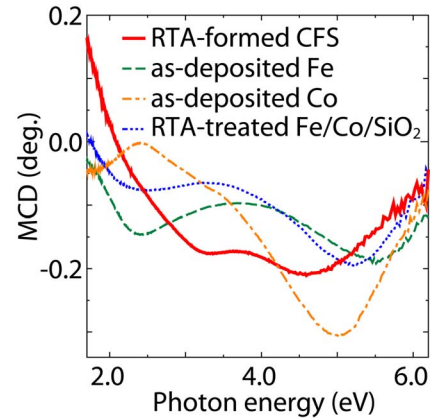
= 700 °C are also shown in the figure as references. All the spectra were measured at room temperature with a reflection configuration with a magnetic field H of 1 T applied perpendicular to the sample plane. In general, a MCD spectrum sensitively reflects the band structure of a material. All the reference samples showed different spectral features, as shown in Fig. 5. The spectral features of the RTA-formed CFS were clearly different from those of reference samples, indicating that the formation of the $L2_1$-phase full-Heusler alloy by the RTA-induced silicidation significantly modified its band structure. In addition, the MCD spectra of the RTA-formed CFS film measured with the several magnitudes of the applied magnetic field exhibited identical magnetic field dependence, i.e., when the intensity of these spectra were normalized, these spectra were completely overlapped with one another. This indicates that the RTA-formed CFS film was magnetically homogeneous; in other words, ferromagnetic precipitates (residual Co, Fe, and other ferromagnetic silicides) can be excluded for the origin of the ferromagnetism in the CFS film.

[1] S. Datta and B. Das, Appl. Phys. Lett. **56**, 665 (1990).
[2] M. Johnson, Science **260**, 320 (1993); IEEE Spectrum **41**, 47 (1994); IEEE Potentials **31**, 26 (1994).
[3] S. Sugahara and M. Tanaka, Appl. Phys. Lett. **84**, 2307 (2004).
[4] S. Sugahara, IEE Proc.: Circuits Devices Syst. **152**, 355 (2005).
[5] R. A. de Groot, F. M. Mueller, P. G. van Engen, and K. H. J. Buschow, Phys. Rev. Lett. **50**, 2024 (1983).
[6] J. M. Larson and J. P. Snyder, IEEE Trans. Electron Devices **53**, 1048 (2006).
[7] K. Inomata, S. Okamura, A. Miyazaki, M. Kikuchi, N. Tezuka, M. Wojcik, and E. Jedryka, J. Phys. D **39**, 816 (2006).
[8] S. Wurmehl, G. H. Fecher, H. C. Kandpal, V. Ksenofontov, C. Felser, H. Lin, and J. Morais, Phys. Rev. B **72**, 184434 (2005).
[9] H. Kijima, T. Ishikawa, T. Marukame, K.-I. Matsuda, T. Uemaru, and M. Yamamoto, J. Magn. Magn. Mater. **310**, 2006 (2007).
[10] R. Nakane, M. Tanaka, and S. Sugahara, Appl. Phys. Lett. **89**, 192503 (2006).
[11] Y. Gao, J. Appl. Phys. **64**, 3760 (1988).
[12] K. H. J. Buschow, P. G. van Engen, and R. Jongebreur, J. Magn. Magn. Mater. **38**, 1 (1983).